Transient Edge Tone Simulation with Convolution Quadrature Boundary Elements

Péter Fiala, Péter Rucz

Budapest University of Technologies and Economics, 1117 Budapest, Hungary, Email: {fiala, rucz}@hit.bme.hu

Introduction

2D transient aeroacoustic simulations are traditionally carried out using acoustic finite elements, where modeling the transient behavior is straightforward, but the radiation condition is not properly fulfilled. As an alternative, the time domain (TD) boundary element method (BEM) can be applied, where the main difficulty lies in the computationally intensive numerical integration and the infinite hold of the time domain Green's function. We present a weakly coupled time domain methodology, where the fluid flow in the vicinity of the object is computed by means of TD finite volumes. Lighthill sources are extracted in the Laplace domain, and the scattering problem is formulated by convolution quadrature BEM, where the computation of the incident acoustic field is accelerated using fast integration methods. As a result, the acoustic response in the far field is given in the time domain. Transient effects, like the resulting sound due to the onset of the incident flow velocity are investigated.

Methodology

Lighthill's analogy expresses the aeroacoustic sound radiation in the form of an inhomogeneous scalar wave equation

$$\nabla^2 p - \frac{1}{c^2}\ddot{p} = -\frac{\partial^2 T_{ij}}{\partial x_i \partial x_j} \tag{1}$$

where p denotes the acoustic pressure, c denotes the speed of sound, and T_{ij} is the Lighthill source tensor, approximated as $T_{ij} = \rho_0 v_i v_j$, where v_i is the i-th component of the fluid velocity and ρ_0 stands for the equilibrium density of air. Assuming zero acoustic velocity on the scatterer boundary Γ (i.e. applying Curle's analogy), as well as zero pressure initial conditions, the following equivalent boundary integral representation (BIR) of the above problem can be formulated:

$$c(x)p(x,t) = \int_0^t \int_\Gamma \frac{\partial G(x,y,t-\tau)}{\partial n_y} p(y,\tau)\mathrm{d}\Gamma_y \mathrm{d}\tau + \int_0^t \int_\Omega G(x,y,t-\tau)\frac{\partial^2 T_{ij}(y,\tau)}{\partial y_i \partial y_j}\mathrm{d}y\mathrm{d}\tau \tag{2}$$

where $G(x,y,t)$ is the fundamental solution of the wave equation, and $c(x)$ is defined as

$$c(x) = \begin{cases} 1 & x \in \Omega \\ 0 & \text{otherwise} \end{cases} \tag{3}$$

Equation (2) explicitly decomposes the pressure into an incident field due to the Lighthill sources, represented by the domain integral, and a scattered field, represented by the boundary integral.

In order to avoid the numerical differentiation of the Lighthill tensor on the domain mesh and improve the accuracy of the numerical integration, Gauss's theorem is applied twice on the domain integral, and the partial derivatives are shifted from T_{ij} to the fundamental solution G. Taking into account that v_i vanishes both on the scatterer boundary (no-slip condition) and in the acoustic target domain (Lighthill's assumption) the following final form of the BIR can be used:

$$c(x)p(x,t) = \int_0^t \int_\Gamma \frac{\partial G(x,y,t-\tau)}{\partial n_y} p(y,\tau)\mathrm{d}\Gamma_y \mathrm{d}\tau + \int_0^t \int_\Omega \frac{\partial^2 G(x,y,t-\tau)}{\partial y_i \partial y_j} T_{ij}(y,\tau)\mathrm{d}y\mathrm{d}\tau \tag{4}$$

Time discretization: convolution quadratures

Temporal discretization of the convolution integrals is performed by means of convolution quadratures. This method, first published by Lubich [1], approximates convolution integrals

$$y(t) = \int_0^t f(t-\tau)g(\tau)\mathrm{d}\tau, \qquad 0 \le t \le T \tag{5}$$

using the discrete form

$$y_k = \sum_{m=0}^{k} \omega_{k-m}(\hat{f}, \Delta t) g_m, \qquad k = 0, \dots, N \tag{6}$$

where $y_k = y(k\Delta t)$ and $g_k = g(k\Delta t)$ denote equidistant samples of the response and the excitation, Δt is the time step, and $\omega_k(\hat{f}, \Delta t)$ denotes the k-th quadrature weight, dependent on the Laplace transformed convolution kernel $\hat{f}$ and the time step. In case of multistep convolution quadratures [1, 2] the weights are computed as

$$\omega_k(\hat{f}, \Delta t) = \frac{1}{2\pi \mathrm{i}} \int_{|z|=\mathcal{R}} \hat{f}\left(\frac{\gamma(z)}{\Delta t}\right) z^{-n-1} \tag{7}$$

where $\hat{f}(s)$ denotes the kernel in the complex frequency domain, $\gamma(z)$ is the quotient of the generating polynomial of a linear multistep method, and the integration radius $\mathcal{R}$ is chosen to be within the domain of analyticity of the kernel $\hat{f}$. An example of the resulting integration path in the s-domain is shown in Figure 1.

Recently, Banjai [3] suggested to define the convolution weights ω_k for negative k indices, practically resulting in $\omega_{-1} = \omega_{-2} \cdots = 0$. Utilizing this redefinition, the upper summation limit k in (6) can be extended to $L-1$ (assuming $L \ge N$), and the following relation is obtained

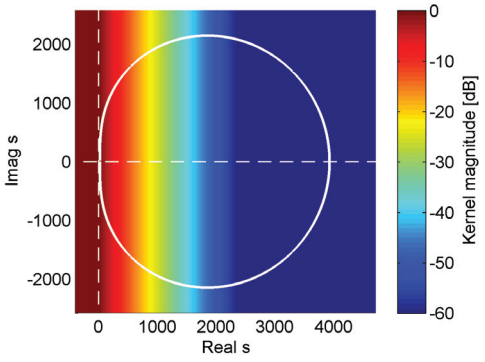

Figure 1: Using convolution quadratures the kernel is evaluated along the path $s = \gamma(z)/\Delta t$ defined by the sampling frequency and the multistep method applied.

between the samples of the excitation g_m and the response y_k:

$$\mathcal{R}^k y_k = \frac{1}{L} \sum_{l=0}^{L-1} \mathrm{e}^{-\mathrm{i}kl2\pi/L} \hat{f}\,(s_l) \sum_{m=0}^{L-1} \mathcal{R}^m g_m \mathrm{e}^{\mathrm{i}ml2\pi/L} \quad (8)$$

Equation (8) defines an efficient transformation method to evaluate the linear convolution in the complex frequency domain. The complex frequency domain representation $\hat{x}(s_l)$ of a discrete time domain function x_k is defined by the transformation pair

$$\hat{x}(s_l) = \sum_{k=0}^{L-1} \mathcal{R}^k x_k \mathrm{e}^{\mathrm{i}kl2\pi/L}, \quad (9)$$

$$\mathcal{R}^k x_k = \frac{1}{L} \sum_{l=0}^{L-1} \hat{x}(s_l) \mathrm{e}^{-\mathrm{i}kl2\pi/L}, \quad (10)$$

and (8) is equivalently expressed by the multiplication $\hat{y}(s_l) = \hat{f}(s_l)\hat{g}(s_l)$.

Convolution quadratures decouple the acoustic scattering problem (4) into independent Helmholtz problems of the form

$$c(x)\hat{p}(x, s_l) = \int_\Gamma \frac{\partial \hat{G}(x, y, s_l)}{\partial n_y} \hat{p}(y, s_l) \mathrm{d}\Gamma_y + \int_\Omega \frac{\partial^2 \hat{G}(x, y, s_l)}{\partial y_i \partial y_j} \hat{T}_{ij}(y, s_l) \mathrm{d}y \quad (11)$$

The excitation and the response can be quickly transformed using a fast Fourier transform. The system is solved separately for each frequency, using well-established elliptic BEM algorithms. This yields a quasi-linear solution method with respect to the number of time steps N. In addition, parallelisation of the solution in the frequency domain is straightforward.

On the other hand, opposed to direct time domain formulations, convolution quadratures are applied for a predefined number of time steps N, and the solution of the acoustic system can only be started after the Lighthill sources were computed and stored for the total time interval. This can require a significant amount of stored data.

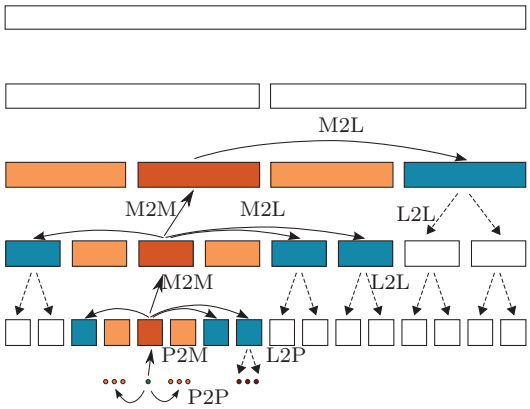

Figure 2: Hieararchical evaluation of low rank approximated kernels in a regular cluster tree.

Fast evaluation of the incident field

Due to the large number of degrees of freedom in the discretized domain Ω, the evaluation of the domain integrals yielding the incident wave field

$$\int_\Omega \frac{\partial^2 \hat{G}(x, y, s_l)}{\partial y_i \partial y_j} \hat{T}_{ij}(y, s_l) \mathrm{d}y \quad (12)$$

is the most expensive part of the numerical procedure regarding computation time. In order to reduce computational costs, fast summation methods need to be applied.

Fast methods can generally be divided into two groups: Kernel-specific and kernel-independent (black-box) methods. Kernel-specific algorithms utilize low rank kernel approximations based on series expansions of the fundamental solution. A common drawback of these methods is that efficient series expansions are obviously kernel-specific, and dedicated algorithms need to be implemented for each fundamental solution. The black-box fast multipole method (FMM), proposed by Fong [4] is a kernel-independent multilevel fast summation method, based on Chebyshev interpolation of the asymptotically smooth kernel. Its extension to oscillating fundamental solutions, the so-called fast directional multilevel summation method was proposed by Messner [5].

The algorithm divides the computation geometry into regular square shaped clusters, forming a quad-tree. The 0-th level cluster contains the whole mesh, higher level clusters are generated by recursively subdividing clusters into four child clusters, until the number of DOF in the leaf cluster is less than a prescribed value.

Two clusters are near to each other if their distance is less than the minimum of their diameters. For the case of near leaf cluster pairs, the integral (12) is evaluated directly (P2P in Figure 2). Interactions between far clusters are evaluated using a low rank approximation of the kernel, consisting of P2M, M2L and L2P interactions.

P2M (point to multipole) interaction consists of aggregating source strengths within a source cluster into a source multipole. For the case of low frequency black box FMM, this operation is Chebyshev anterpolation from

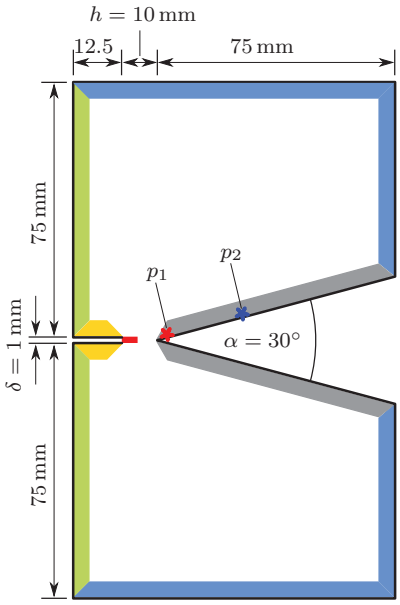

Figure 3: CFD geometry and boundary conditions.

the source nodes to Chebyshev nodes of the containing source cluster. M2L stands for multipole to local translation, where the kernel is directly evaluated between the Chebyshev nodes of the source and receiver clusters. Finally, L2P describes local to point operation, where the receiver field is interpolated from the Chebyshev nodes of the receiver cluster to the receiver points.

For the case of a regular cluster tree, the applied black box FMM is advantageous, as the M2M and L2L interactions are described by a single level-independent interpolation matrix and its transpose. Furthermore, exploiting the translation invariance of the kernel, M2L interactions (kernel evaluations) need to be computed and stored only between a small number of source–receiver cluster pairs. Finally, as the P2M and M2M operations are frequency independent, source clusters that do not take part in near field interactions can be aggregated directly in the time domain. This results in a significant compression of the time domain excitation data.

Edge tone CFD simulation

The configuration reported in [6] and shown in Figure 3 was chosen for the flow simulation. No-slip condition, i.e. $v_i = 0$ was defined on the wedge walls (gray), while free-slip was defined on the rigid nozzle walls (yellow). Free flow (outlet–inlet) boundary condition was prescribed on the free boundaries (blue). The inlet flow velocity (red) had a transient top hat profile, with the velocity increasing slowly from zero to 3.1 m/s. This corresponds to a maximal Reynolds number of $\mathrm{Re}_{\max} = 200$. On the free boundary behind the nozzle (green), a support flow was defined with 1% of the inlet velocity.

An unstructured mesh consisting of 40,378 wedge elements was used in the simulations. In order to provide sufficient spatial resolution for the CFD solution the mesh was very fine in the vicinity of the tip. The CFD simulation was performed using the `pisoFoam` solver of `OpenFOAM-2.3`. The total simulated time was 1,250 ms, and the resulting velocity and pressure fields were exported with a sampling frequency of 2 kHz.

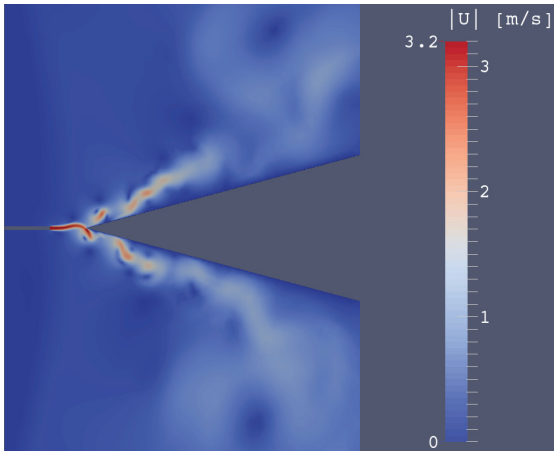

Figure 4: Snapshot of the velocity field at $t = 1{,}250$ ms.

Figure 4 displays the snapshot of the simulated velocity field at the time instance $t = 1{,}250$ ms. The oscillation of the air jet around the wedge and the resulting vortices are clearly visible. Figure 5 shows the time history and frequency content of the pressure forces acting on the wedge. The time history shows the onset of the pressure force, whereas the spectrum was evaluated in the steady state. The oscillation starts around $\mathrm{Re} \approx 100$. Apparently, the pressure force shows two strong tonal components: the fundamental frequency at 115 Hz and its third harmonic.

Results of the acoustic computation

The acoustic scatterer boundary mesh was defined as the continuation of the wedge to a total length of 0.5 m. The highly irregular mesh consists of 1,000 linear line elements. The edge size increases from 70 μm to 2.5 mm with the distance from the tip.

The regular quad tree containing the triangular elements of the fluid mesh and the line elements of the scatterer mesh consists of a total number of 10,000 clusters whithin a non-balanced cluster tree with a maximal depth of 12. M2L interactions were computed between 25,534 cluster pairs, but due to the regularity of the quad-tree, only 1,575 uniquely oriented cluster pairs needed to be processed. The fast summation method allowed to reduce the total number of kernel evaluations to 2%. The numerical calculations were performed using the open source C++ BEM toolbox NiHu [7].

Figure 6(a) displays the resulting acoustic pressure in two points of the scatterer. The locations of the two points are displayed in Figure 3. As the Lighthill sources are proportional to the square of the flow velocity, the second harmonic at $f = 230$ Hz appears in the acoustic pressure field. Regarding the time history of the acoustic pressure onset, the results show similar development as the pres-

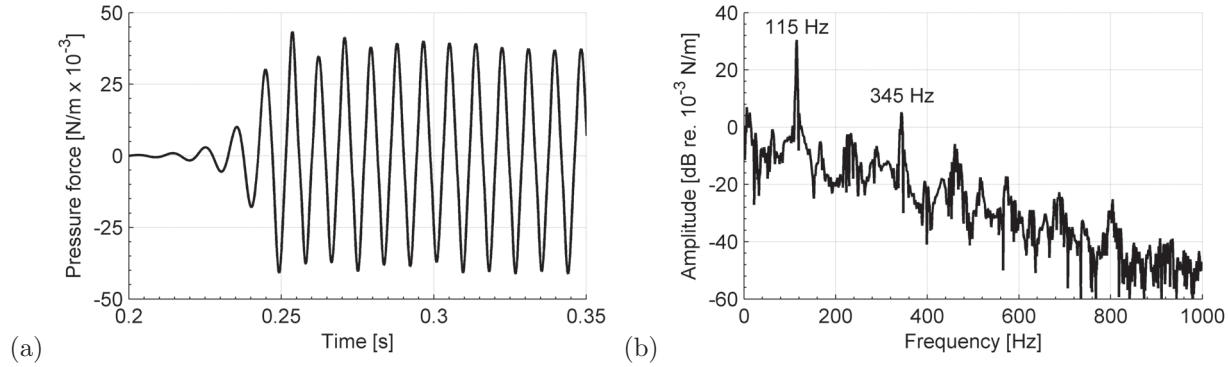

Figure 5: Time history (a) and frequency content (b) of the pressure forces acting on the wedge.

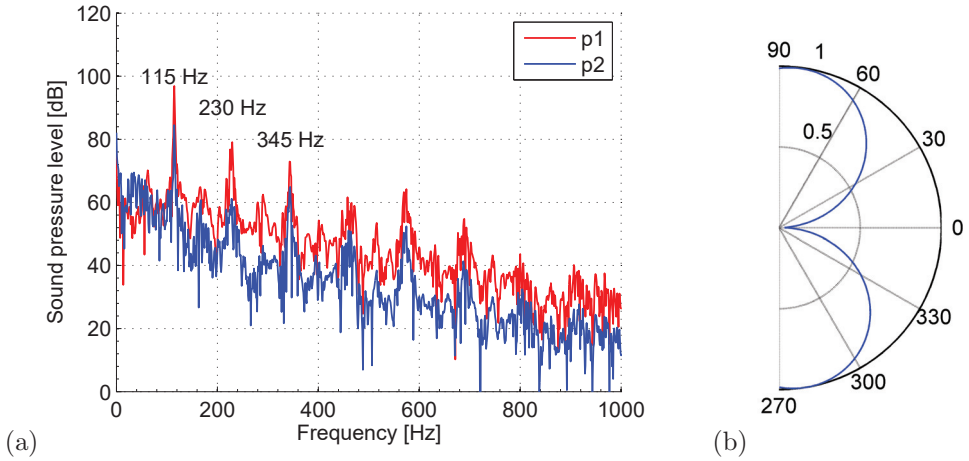

Figure 6: (a) Frequency content of the acoustic pressure evaluated in two points of the scatterer. (b) Far-field steady state directivity pattern of the edge tone evaluated at a distance of $R = 3\,\mathrm{m}$ from the tip.

sure forces. Figure 6(b) displays the directivity pattern of the edge tone, evaluated based on the magnitude of the steady state far-field acoustic pressure. The directivity was evaluated along a circle of 3 m radius, centered at the tip. The resulting typical dipole characteristics is in good agreement with the expectations.

It was observed that the onset of the inlet velocity has a significant effect on the resulting flow field and hence the radiated sound. Based on the results of the reference case discussed above it can be assessed that the proposed methodology is cabable of reproducing more complex transient aeroacoustic phenomena too, such as hysteretic behavior (see Ref. [6]). Examination of such configurations is among the future plans of the authors.

Conclusions

A computational framework was set up that is capable of simulating transient aeroacoustic problems using integral equation methods. With the application of convolution quadratures the acoustic simulation is performed in the complex frequency domain. This allows the application of conventional fast integration methods for the evaluation of the Lighthill sources. Application of the low frequency black box FMM results in a significant acceleration of the solution process, and also in a remarkable compression of the excitation data in the time domain.

References

[1] C. Lubich. Convolution quadrature and discretized operational calculus. I. *Numerische Mathematik*, 52:129–145, 1988.

[2] M. Schanz and H. Antes. Application of 'operational quadrature methods' in time domain boundary element methods. *Meccanica*, 32:179–186, 1997.

[3] L. Banjai and S. Sauter. Rapid solution of the wave equation in unbounded domains. *SIAM Journal of Numerical Analysis*, 47(1):227–249, 2008.

[4] W. Fong and E. Darve. The black-box fast multipole method. *Journal of Computational Physics*, 228:8712–8725, 2009.

[5] M. Messner, M. Schanz, and E. Darve. Fast directional multilevel summation for oscilatory kernels based on Chebyshev interpolation. *Journal of Computational Physics*, 231(4):1175–1196, 2012.

[6] Gy. Paál and I. Vaik. Unsteady phenomena in the edge tone. *International Journal of Heat and Fluid Flow*, 28:575–586, 2007.

[7] P. Fiala and P. Rucz. NiHu: an open source C++ BEM library. *Advances in Engineering Software*, 75:101–112, 2014.